Supporting Information

Plasma Induced Transformation：A New Strategy to *in situ* Engineer MOF-derived Heterointerface for High-Efficiency Electrochemical Hydrogen Evolution

Xin Kong[b], Guiyang Liu[c], Hui-Qing Peng[a], Zian Xu[b], Shuyu Bu [b], Bin Liu [a,], and Wenjun Zhang[b,d,]**

[a]*State Key Laboratory of Chemical Resource Engineering, Beijing University of Chemical Technology, Beijing 100029, China.*

[b]*Center of Super-Diamond and Advanced Films (COSDAF) and Department of Materials Science and Engineering, City University of Hong Kong, HK SAR, China.*

[c]*Lab of New Materials for Power Sources, Honghe University, Mengzi, Yunnan, China.*

[d]*City University of Hong Kong Shenzhen Research Institute, Shenzhen 518057, China*

Corresponding author. Email: binliu@buct.edu.cn (B. Liu); apwjzh@cityu.edu.hk (W. Zhang)

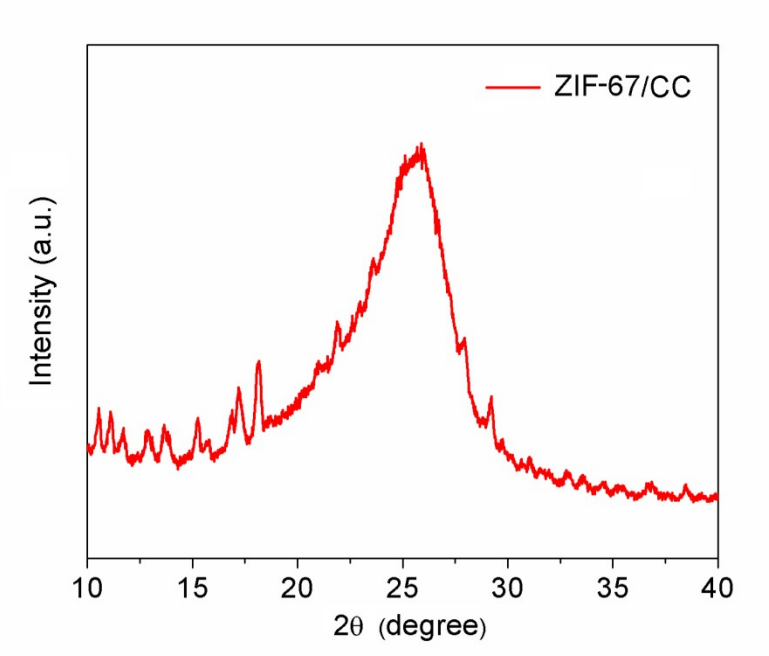

Fig. S1. XRD pattern of ZIF-67/CC.

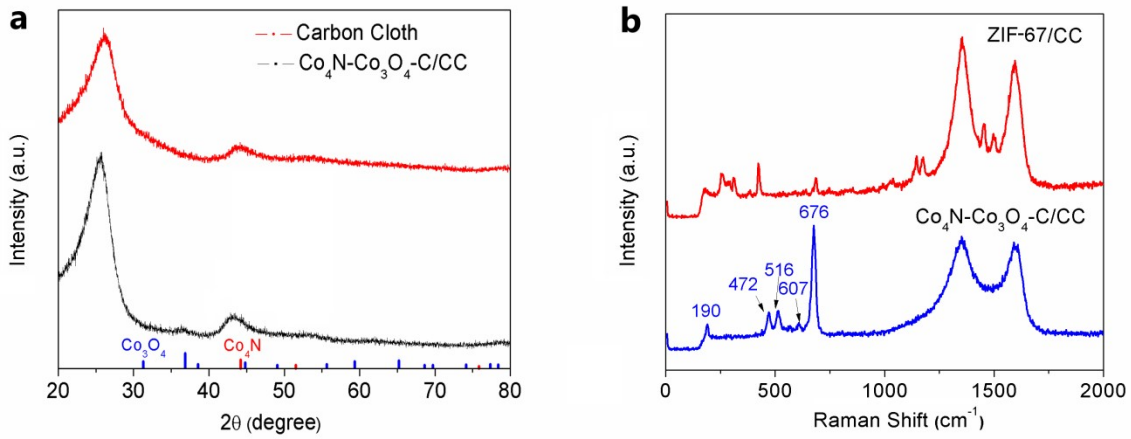

Fig. S2. (a) XRD patterns of CC and Co_4N-Co_3O_4-C/CC, and (b) Raman spectra of ZIF-67/CC and Co_4N-Co_3O_4-C/CC.

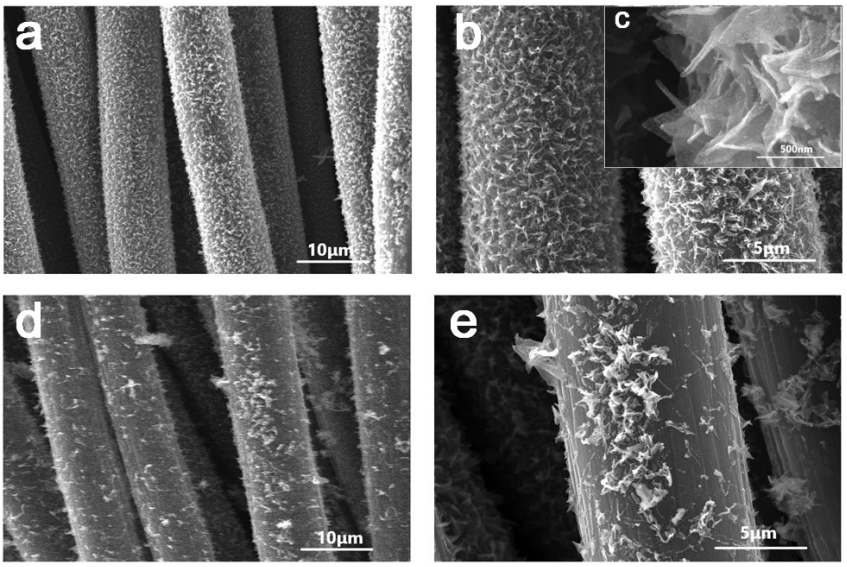

Fig. S3. SEM images of (a)-(c) Co_4N-Co_3O_4-C/CC-1, (d) and (e) Co_4N-Co_3O_4-C/CC-10.

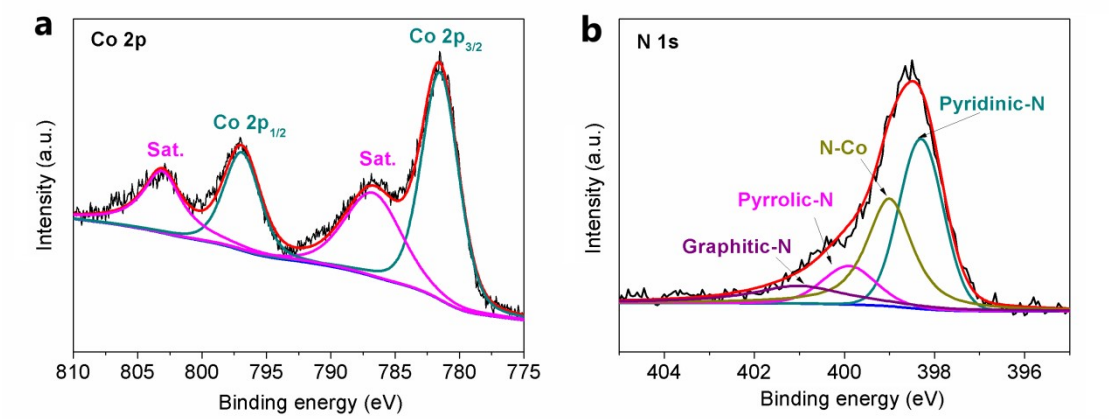

Fig. S4. High-resolution XPS spectra of (a) Co 2p and (b) N 1s of Co_4N-C/CC.

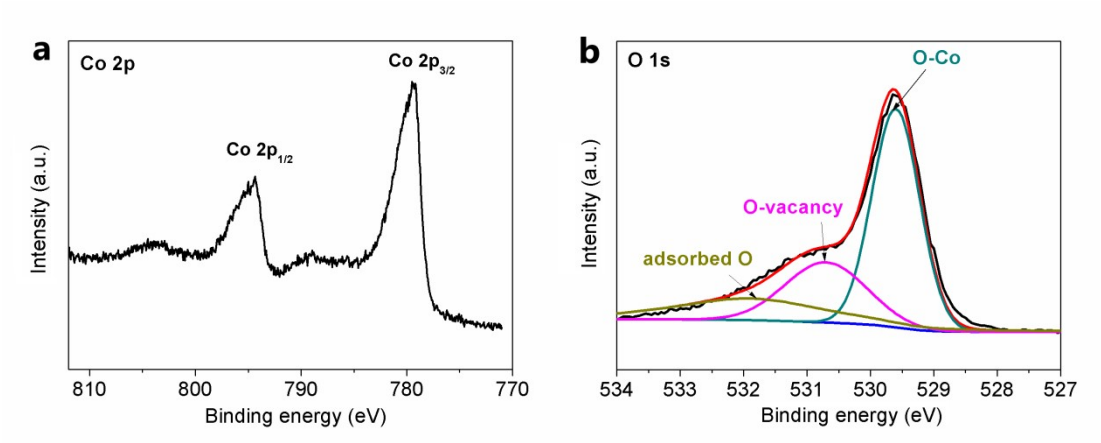

Fig. S5. High-resolution XPS spectra of (a) Co 2p and (b) O 1s of Co_3O_4-C/CC.

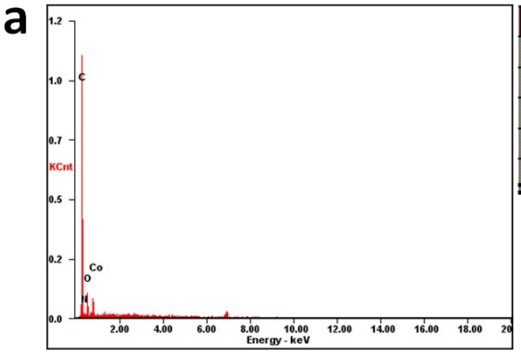

Element	Wt%	At%
CK	68.96	83.44
NK	03.73	03.87
OK	08.99	08.16
CoL	18.33	04.52
Matrix	Correction	ZAF

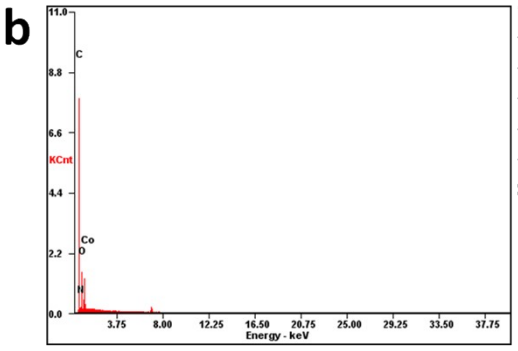

Element	Wt%	At%
CK	54.88	74.24
NK	06.04	07.00
OK	10.79	10.96
CoL	28.29	07.80
Matrix	Correction	ZAF

Fig. S6. EDX results of (a) Co_4N-Co_3O_4-C/CC-1 and (b) Co_4N-Co_3O_4-C/CC-5.

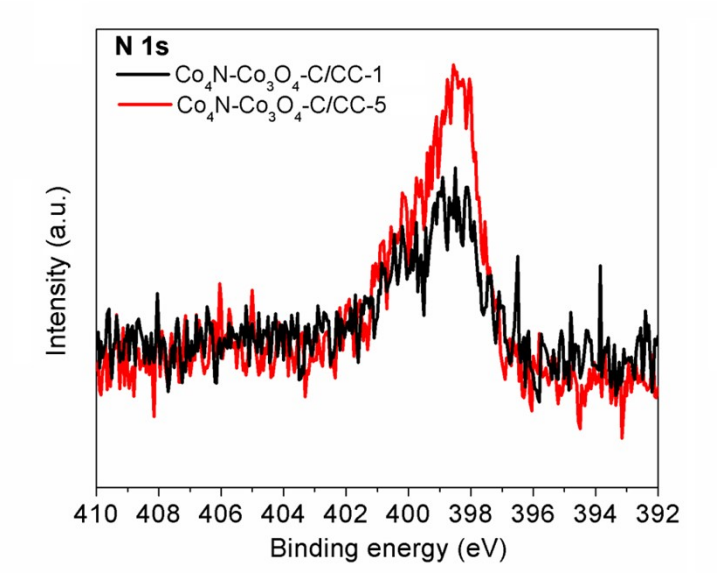

Fig. S7. High-resolution XPS spectra of N 1s collected on Co_4N-Co_3O_4-C/CC-1 and Co_4N-Co_3O_4-C/CC-5.

The nitrogen atomic percentages of Co_4N-Co_3O_4-C/CC-1 and Co_4N-Co_3O_4-C/CC-5 are 4% and 7% according to the XPS analysis which is similar with EDX results. When the plasma treatment is prolonged to 10 min, the sample material is almost etched away from carbon cloth and the surface of carbon cloth becomes smooth again, which results in that the high-resolution XPS spectra of N 1s collected on Co_4N-Co_3O_4-C/CC-10 cannot be used to compare with those on Co_4N-Co_3O_4-C/CC-1 and Co_4N-Co_3O_4-C/CC-5. Therefore it is not shown in **Fig. S7**.

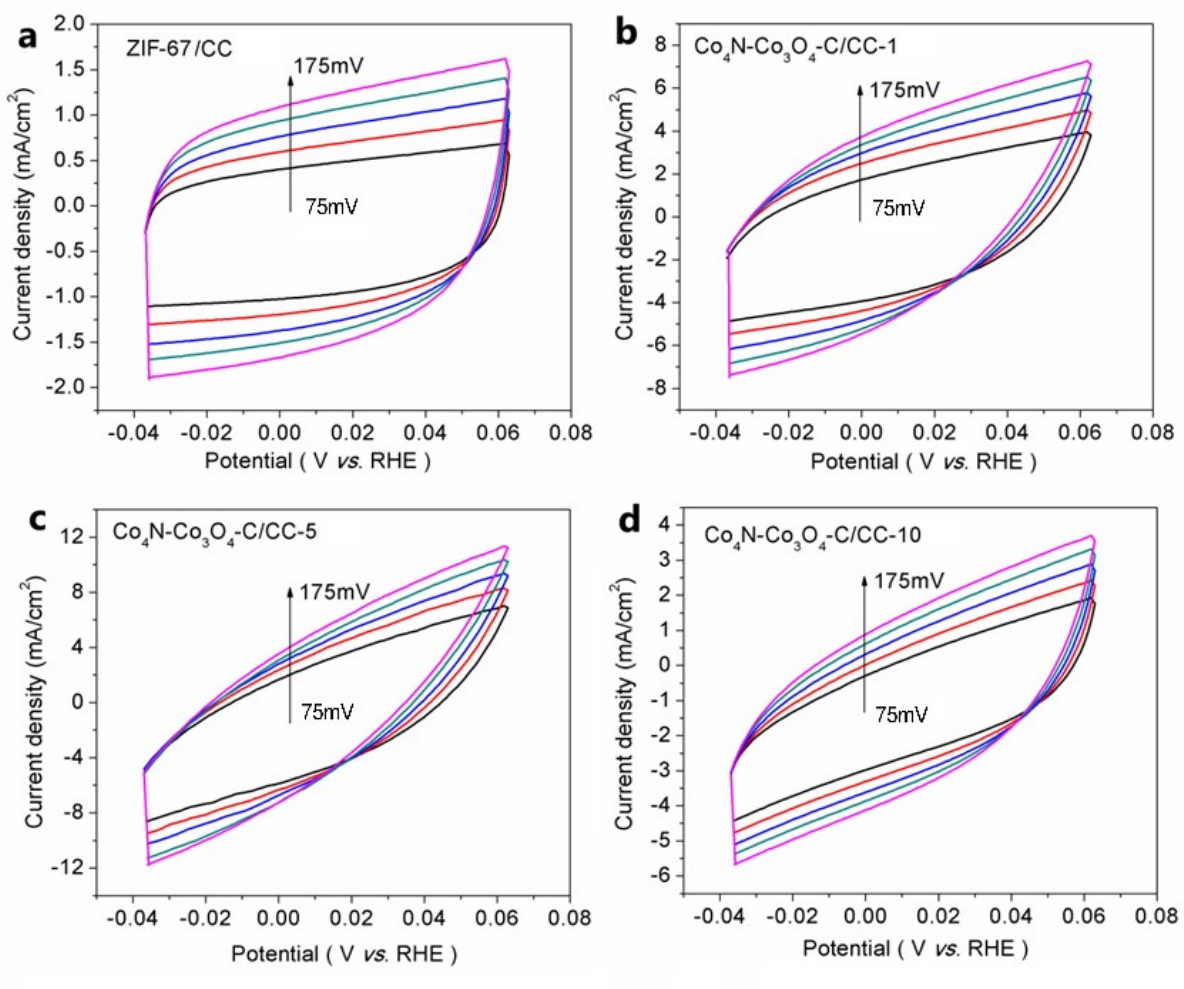

Fig. S8. The CV curves of (a) ZIF-67/CC, (b) Co_4N-Co_3O_4-C/CC-1, (c) Co_4N-Co_3O_4-C/CC-5, and (d) Co_4N-Co_3O_4-C/CC-10 measured at different scan rates of 75, 100, 125, 150, and 175 mV s^{-1} in KOH solution.

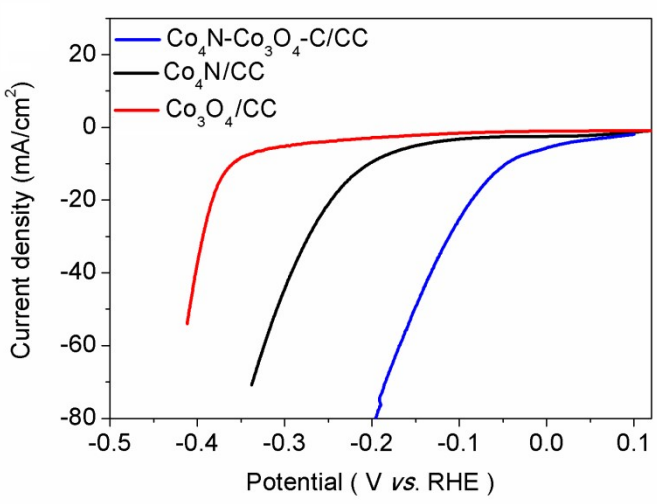

Fig. S9. The LSV curves of Co_4N-Co_3O_4-C/CC-5, control samples Co_4N/CC and Co_3O_4/CC.

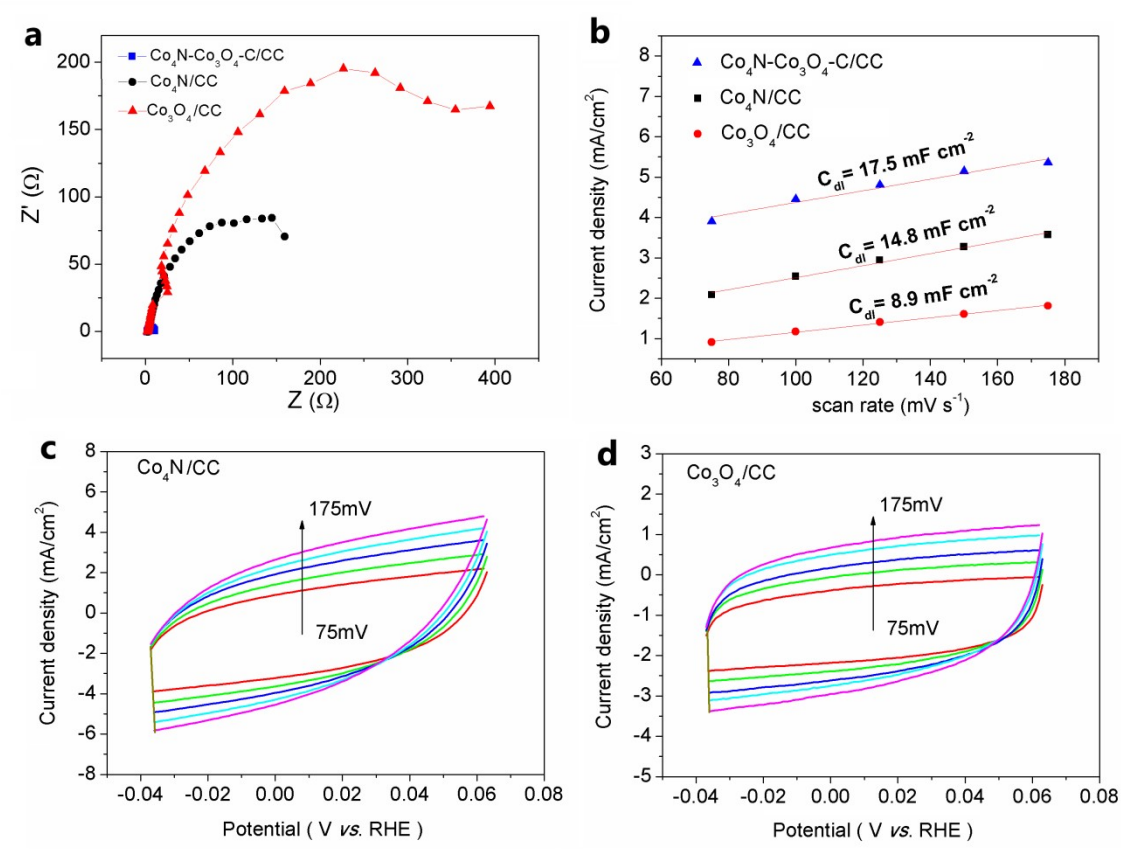

Fig. S10. (a) The Nyquist plots of Co_4N-Co_3O_4-C/CC-5, control samples Co_4N/CC and Co_3O_4/CC obtained from the EIS measurements. (b) The linear fitting of the capacitive currents of the electrodes as a function of scan rates. The CV curves of (c) Co_4N/CC and (d)

Co_3O_4 /CC measured at different scan rates of 75, 100, 125, 150, and 175 mV s^{-1} in KOH, respectively.

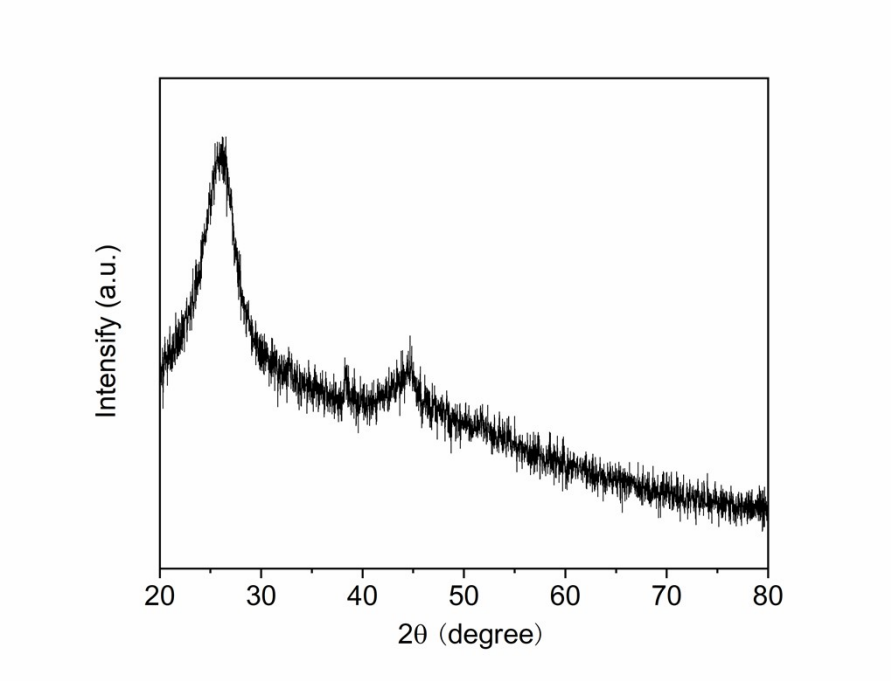

Fig. S11. XRD pattern of Co_4N-Co_3O_4-C/CC-5 after HER stability measurement for 140 h in 1.0 M KOH solution.

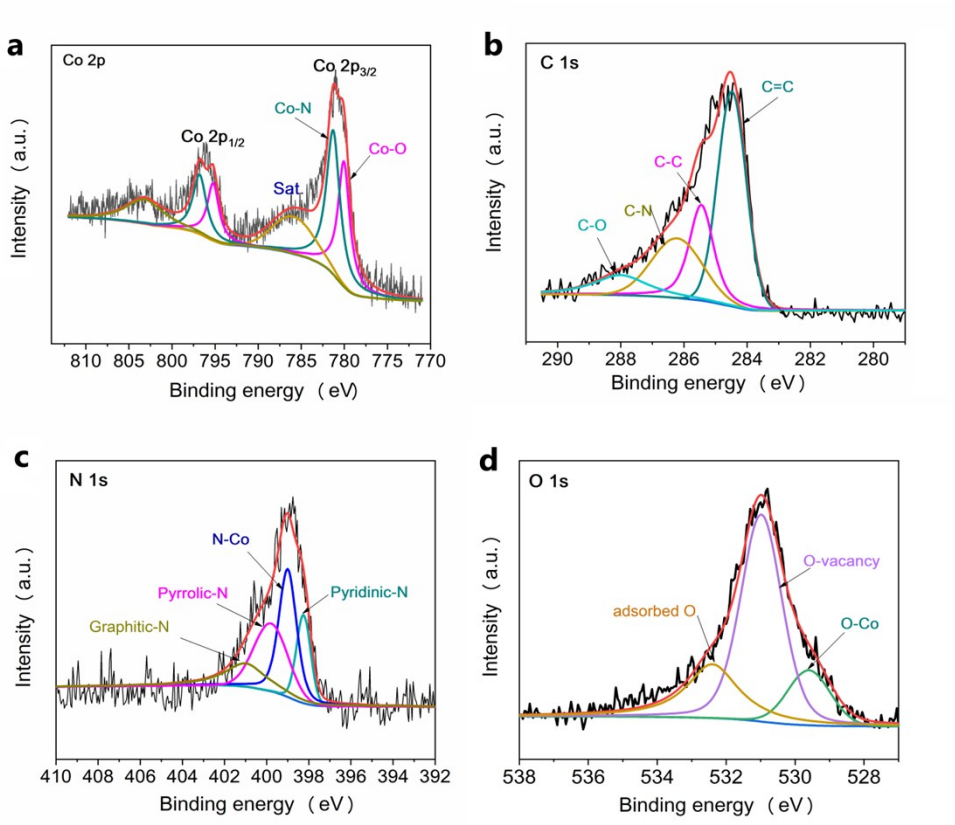

Fig. S12. High-resolution XPS spectra and deconvolutions of (a) Co 2p, (b) C 1s, (c) N 1s and (d) O 1s of Co_4N-Co_3O_4-C/CC-5 after HER stability measurement for 140 h in 1.0 M KOH solution.

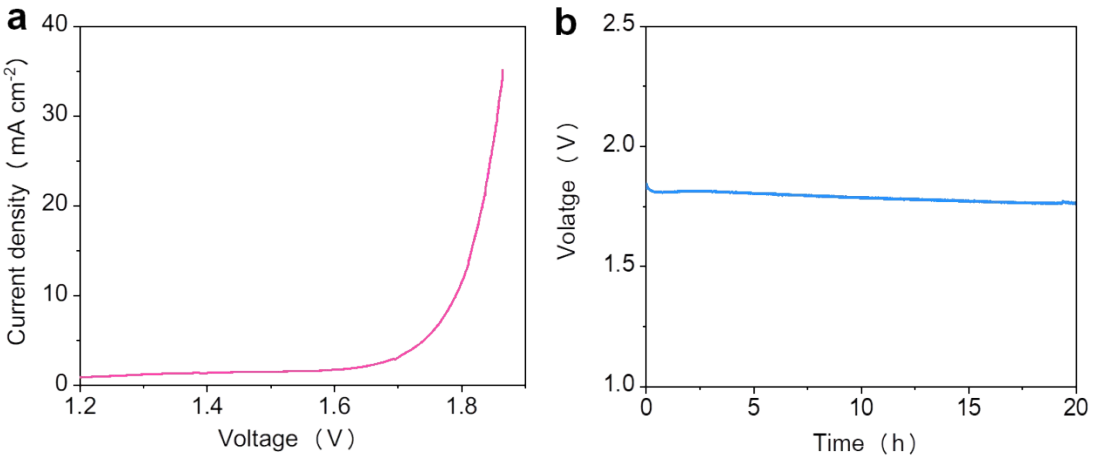

Fig. S13. (a) The LSV curve and **(b)** chronopotentiometry curve at 10 mA cm^{-2} of AWE system.